Lasing, trapping states, and multistability in a circuit quantum electrodynamical analog of a single-atom injection maser

Michael Marthaler, Juha Leppäkangas, and Jared H. Cole

Institut für Theoretische Festkörperphysik and DFG–Center for Functional Nanostructures (CFN), Karlsruhe Institute of Technology,

D-76128 Karlsruhe, Germany

We study a superconducting single-electron transistor (SSET) which is coupled to a *LC* oscillator via the phase difference across one of the Josephson junctions. This leads to a strongly anharmonic coupling between the SSET and the oscillator. The coupling can oscillate with the number of photons, which makes this system very similar to the single-atom injection maser. However, the advantage of a design based on superconducting circuits is the strong coupling and existence of standard methods to measure the radiation field in the oscillator. This makes it possible to study many effects that have been predicted for the single-atom injection maser in a circuit quantum electrodynamics setup.

Introduction. The ability to fabricate and control superconducting quantum circuits has given birth to the field of circuit quantum electrodynamics (circuit QED). Within these circuits, quantized charge, superconducting phase difference, and even individual microwave photons can be controlled and manipulated, introducing the idea of "artificial" atom-photon physics. Such circuits have been used to reach the strong-coupling regime,[1,2] observe heating and cooling,[3,4] realize a three-level-laser,[5–7] and make great strides forward in creating highly tunable "artificial" atoms coupled to an oscillator.[8] A number of proposals[9,10] and ultimately experiments[4,7] have realized the idea of a linearly coupled single "artificial-atom" laser (or more precisely maser). Such work strives toward a circuit analogy of the experimental generation of coherent microwave radiation using single-atom masers.[11–13]

Despite much progress, several important physical effects that have been painstakingly studied in single-atom injection masers have yet to be realized in circuit QED. These effects include multistability of the cavity field[14] and trapped photon numbers states.[15] In all these experiments, the state of the system is inferred via measurement of the excited state occupancy of Rydberg atoms as they drop through a microwave cavity.

In this Rapid Coummincation we will investigate a superconducting single-electron transistor (SSET) coupled to a *LC* oscillator via the phase difference across the SSET's right-hand Josephson junction (JJ). In doing so, we show that this device allows one to reach a regime of strongly nonlinear coupling. It displays multistability and trapping states, as well as possesses an operating point which reduces noise from low-frequency charge fluctuations. As such, this device provides a close analogy to the single-atom injection experiments of cavity QED. However, in contrast to previous experiments, a circuit-QED setup allows the direct detection of the photon state of the resonator via time-resolved measurements of the emitted microwave radiation.

The system. One realization of our desired circuit is the series coupling of the oscillator with the SSET [Fig. 1(a)]. Another option is the more conventional inductive coupling scheme[4] [Fig. 1(b)]. We divide the coherent Hamiltonian into three parts, describing the artificial atom, the photon mode, and the interaction between them:

$$H_0 = H_{\text{atom}} + H_{\text{int}} + H_{\text{photon}}. \tag{1}$$

In both realizations the artificial atom, which forms the basis of the micromaser, is provided by the charge on the SSET island and Cooper-pair tunneling across the left JJ and is described by the Hamiltonian

$$H_{\text{atom}} = 4E_C(N - N_G)^2 - E_{JL}\cos(\phi_L). \tag{2}$$

Here E_{JL} is the corresponding Josephson coupling and the charge on the island, $2eN$, and the phase difference ϕ_L across the left JJ satisfy the periodic commutation relation $[N, e^{\pm i\phi_L}] = \pm e^{\pm i\phi_L}$. The explicit forms of the gate charge N_G and the charging energy E_C depend on the realization and are given below explicitly for the series coupling. The gate voltage U is used to bias the system such that single-Cooper-pair tunneling is resonant across the left JJ. The quantized mode can always be described as a harmonic oscillator ($\hbar = 1$), $H_{\text{photon}} = \omega_0 a^\dagger a$.

For the series coupling scheme the interaction Hamiltonian between the atom and the cavity has the form

$$H_{\text{int}} = -E_{JR}\{\cos(2eVt + \phi_L)\cos[\mathcal{G}(a + a^\dagger)] \tag{3}$$
$$- \sin(2eVt + \phi_L)\sin[\mathcal{G}(a + a^\dagger)]\} + H_{\text{cc}},$$

where E_{JR} is the Josephson coupling across the right-hand JJ and we have used the condition that the phase difference across the SSET and the oscillator is fixed by the transport voltage V, similar to the approach used in Ref. 16. As we will discuss in more detail later the coupling term $\sin[\mathcal{G}(a^\dagger + a)]$ will provide the anharmonic coupling that makes our system similar to the single-atom injection maser. Additionally, we have a capacitive coupling term,

$$H_{\text{cc}} = -\frac{2iE_{\text{cc}}}{\mathcal{G}}N(a^\dagger - a). \tag{4}$$

The important coupling constant is $\mathcal{G} = (2\epsilon_C/E_L)^{1/4}$, where $\epsilon_C = e^2\bar{C}_\Sigma/2C_\Sigma^2$, $\bar{C}_\Sigma = C_G + C_L + C_R$, $C_\Sigma^2 = (C_G + C_L)C_R + C\bar{C}_\Sigma$, and E_L is the magnetic energy of the inductor (with capacitances defined in Fig. 1). The fact
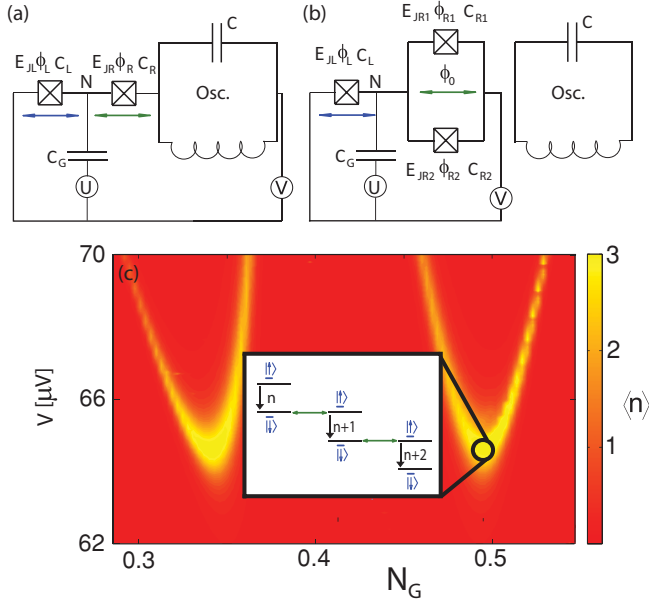
FIG. 1. (Color online) (a) The superconducting single-electron transistor (SSET) in series with the LC oscillator. The SSET consists of two Josephson junctions (crossed boxes) with a capacitively connected gate on the small island in between. (b) Illustration of the inductive coupling scheme, where a SQUID forms an effective right-hand JJ and is thread by the bias flux ϕ_0 and the oscillator flux $i\mathcal{G}(a^\dagger - a)$. (c) The photon number $\langle n \rangle$ in the oscillator [setup (a)] as a function of the gate charge $N_G \propto U$ and the transport voltage V. A symmetry point of particular interest is circled. For our discussion of the regime of strongly nonlinear coupling, we restrict ourselves to this symmetry point. The parameters of the simulation are $E_{JL} = E_{JR} = 30\ \mu\text{eV}$, $\omega_0 = 24$ GHz, $C_L = C_R = 40C_G = C/1250 = 0.4$ fF ($\mathcal{G} = 0.08$), $T = 50$ mK, and $R_U = R_V = 100\ \Omega$, and the oscillator has a decay rate of $\kappa = 12$ MHz.

that it is possible to construct circuits where the coupling constant $\mathcal{G}$ can be rather big, $\mathcal{G} \lesssim 1$, is the crucial ingredient in reaching the strongly nonlinear coupling limit. The charging energy of the SSET island is $E_C = (C + C_R)e^2/2C_\Sigma^2$, the strength of the capacitive coupling is characterized by $E_{cc} = e^2 C_R/C_\Sigma^2$, and the gate charge has the form $N_G = \{V[C_R/(C + C_R)][C + C_R(C_G + C)/\bar{C}_\Sigma] - U[C_G - C_R^2 C_G/((C + C_R)\bar{C}_\Sigma)]\}/2e$. The inductive coupling provides the same anharmonic coupling as given by Eq. (3). However, the coupling strength $\mathcal{G}$ depends on the geometry of the system and in most cases remains small ($G \ll 1$). Finally, the frequency of the oscillator is $\omega_0 = \sqrt{8\epsilon_C E_L}$.

Directionality of our lasing cycle is created through the standard 100 ohm noise in the voltages. It effectively leads to fluctuations $V \to V + V_f$ and $U \to U + U_f$ described by the Hamiltonian H_{EE} and characterized by equilibrium correlations of the form

$$\langle U_f(t)U_f(0)\rangle = \frac{R_U}{\pi}\int_{-\infty}^{\infty} d\omega \frac{\omega}{1 + \left(\frac{\omega}{\omega_c}\right)^2}\frac{e^{-i\omega t}}{1 - e^{-\beta\omega}}, \quad (5)$$

where R_U is the resistance in the gate line and the cutoff $\omega_c = 1/R_U C_U \gg \omega_0$. At the relevant frequencies ($\omega \gg k_B T$) the noise is asymmetric with respect to absorption and emission of energy. The Hamiltonian of the total system is[17] $H_T =$

$H_0 + 2eN_V V_f + 2eN_U U_f + H_{\text{EE}}$, where the coupling of the voltage fluctuations to SSET and oscillator is mediated by the operators N_V and N_U. For the series LC oscillator one obtains

$$N_U = -\frac{i}{2}\frac{C_G C_R}{C_\Sigma^2}\frac{a^\dagger - a}{\mathcal{G}} + \left[\frac{C_G(C + C_R)}{C_\Sigma^2} - \frac{C_R^2 C_G}{C_\Sigma^2 \bar{C}_\Sigma}\right]N.$$

Similar relations apply for transport voltage fluctuations V_f and the interaction operator N_V. As one can see for series coupling we create additional noise in the oscillator as well. We will always include this effect by using an oscillator decay rate which will be larger than the decay induced only by the voltage fluctuations to allow for additional internal or external loss.

For the remainder of this Rapid Communication, we focus on the series coupling scheme [Fig. 1(a)] as this allows a stronger nonlinear coupling between qubit and oscillator, but our results apply to both schemes. To be able to study the system in all generality we extend the complete model of the SSET as discussed in Ref. 17 to include the photon number states of the oscillator. We diagonalize the Hamiltonian (1) using the Floquet expansion of the eigenstates, $|\psi\rangle = \sum_{n,n',N} c_{nn'N} e^{2in'e\tilde{V}t}|n\rangle|N\rangle$, where $|n\rangle$ are the photon number states of the oscillator and $|N\rangle$ are the charge states of the island. We then treat the voltage fluctuations perturbatively by expanding the time evolution of the resulting density matrix in orders of the coupling to the reservoirs. After tracing out the reservoir degrees of freedom we arrive at the Bloch-Redfield equation for the reduced density matrix ρ of the system.

Cascade resonance. In Fig. 1(c) we plot the average photon number as a function of the gate charge N_G and transport voltage V for our device, obtained using a full density-matrix simulation of the SSET and oscillator. Several resonances appear at different regions in the V-N_G plane shown in Fig. 1(c). These points correspond to a resonance condition between levels of the SSET and the oscillator. We focus our further discussion on the symmetry point at $N_G = 1/2$, where the charge states $|N = 0\rangle$ and $|N = 1\rangle$ are degenerate. At this symmetry point we are able to qualitatively describe features of the system by a simplified master equation. We will now discuss the relevant terms in this equation and explain how a lasing cycle can be achieved.

The eigenstates of the effective atom are given by the qubit states: symmetric and antisymmetric superposition of the degenerate charge states $|\downarrow\rangle$ and $|\uparrow\rangle$, respectively. The energy splitting is given by $\Delta E = E_{JL}$. Close to the symmetry point the energy changes with $(N_G - 1/2)^2$ and is therefore protected to the first order from low-frequency charge noise.[18] After we perform the transformation $U = \exp[-i2eV a^\dagger a t]$ and the rotating-wave approximation, our Hamiltonian becomes

$$H_U = \frac{1}{2}\Delta E \sigma_z - \omega_{\text{eff}} a^\dagger a + \frac{i E_{JR}}{2}[\sigma_+ s_+ - \sigma_- s_-], \quad (6)$$

with an effective oscillator frequency $\omega_{\text{eff}} = 2eV - \omega_0$ and the operators $s_+ = \sum_n \langle n + 1|\sin[\mathcal{G}(a^\dagger + a)]|n\rangle|n + 1\rangle\langle n|$ and $s_- = s_+^\dagger$. At the symmetry point that is circled in Fig. 1(c) we have $2eV > \omega_0$. This means that in our rotating frame each photon that is created effectively decreases the energy of the system.

Charge noise allows decay from the qubit state $|\uparrow\rangle$ to the qubit ground state $|\downarrow\rangle$. This in turn creates a higher population in the state $|\downarrow\rangle$. If the resonance condition $\omega_0 = 2eV - \Delta E$ ($\Delta E = \omega_{\text{eff}}$) is fulfilled there is a coherent transition between $|\downarrow\rangle|n\rangle$ and $|\uparrow\rangle|n+1\rangle$. Through this mechanism photons are created in a cascade of energy decay and absorption of voltage quanta [see schematic in Fig. 1(c)].

At the symmetry point we can write the master equation in a simplified Lindblad form,

$$\dot{\rho} = -i[H_U, \rho] + \mathcal{L}_{\text{ch}}\rho + \mathcal{L}_{\text{diss}}\rho, \tag{7}$$

with the standard Lindblad operator for the oscillator decay with rate κ and qubit decay,

$$\mathcal{L}_{\text{ch}}\rho = \gamma(\sigma_-\rho\sigma_+ - [\sigma_+\sigma_-, \rho]_+/2), \tag{8}$$

where $[,]_+$ is the anticommutator, and the decay rate is given by

$$\gamma = \sum_{k=U,V} |\langle\downarrow|2eN_k|\uparrow\rangle|^2 \int_{-\infty}^{\infty} dt \langle k_f(t)k_f(0)\rangle e^{i\Delta E t}. \tag{9}$$

This decay rate corresponds to $1/T_1$ in a charge qubit. The overall form of our master equation is now significantly simplified and similar to the master equation of a single-atom injection maser. In the rotating-wave approximation used to derive the Hamiltonian (6) we neglected many matrix elements connecting different photon number states. However, comparison to our full solution shows that all qualitative features of the system are well described by Eq. (7).

Anharmonic coupling. The key difference between this circuit and existing circuit-QED setups is the anharmonic coupling term, $\sin[\mathcal{G}(a^\dagger + a)]$. To understand the effects of this term, we consider three different regimes. Expanding the anharmonic term for weak coupling $\mathcal{G} \ll 1$, we obtain a linear coupling $s_+ \approx \mathcal{G}a^\dagger$, resulting in the usual single-qubit lasing results.[3,5,6] In this case we find the photon number at resonance, $\omega_{\text{eff}} = \Delta E = E_{JL}$, to be[19] $\langle n \rangle_0 = \gamma/2\kappa - \gamma^2/2(E_{JR}\mathcal{G})^2$ for $\langle n \rangle_0 \gg 1$. This expression for the photon number in the linear coupling limit will prove to be useful in understanding the other regimes that we can reach using this device.

An advantage of this circuit is that we are not limited to the linear coupling regime. As the strength of the effective coupling term is roughly sinusoidal with $\mathcal{G}$ and photon number, we see a number of new effects. Ironically, when operating in this mode, our micromaser behaves in a very similar fashion to a single-atom injection maser,[11,14,15] where our oscillatory coupling provides a direct analog to the spatially dependent atom-field coupling in injection masers. In Fig. 2 one can see the probability distribution of the photon number states, $\rho_n = \langle n| \text{Tr}_{\uparrow/\downarrow}[\rho]|n\rangle$, in the stationary limit $\dot{\rho} = 0$, as a function of the coupling strength $\mathcal{G}$. As discussed above, for small coupling (marked by I) we simply get the Poisson distribution we would expect for a laser.[19]

For slightly larger coupling (or photon number) we obtained a squeezed number distribution within the oscillator. This regime (II) is reached when $\pi/2 \lesssim \mathcal{G}\sqrt{\langle n\rangle_0} \lesssim \pi$. If this condition is fulfilled, as the photon number approaches the upper limit ($\mathcal{G}\sqrt{\langle n\rangle_0} \to \pi$), the matrix element s_+ is effectively cut off, resulting in the usual squeezed state physics.[9,10] This can
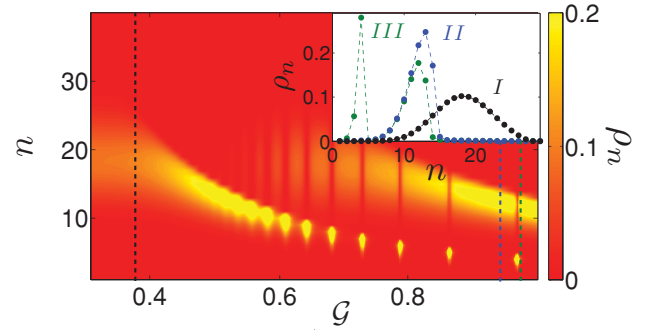
FIG. 2. (Color online) The photon distribution ρ_n as a function of the coupling strength $\mathcal{G}$, where we keep the linear coupling strength $E_{JR}\mathcal{G}$ constant. We see three major types of behavior, each of which we show in the inset: a Poisson distribution for small coupling (black, I) and for increasing $\mathcal{G}$ a squeezed distribution (blue, II) and multistability (green line, III). We used the parameters $\kappa/\gamma = 0.027$ and $\mathcal{G}E_{JR}/\gamma = 6.7$.

be seen in the asymmetric character of the photon number distribution (the blue curve) in the inset to Fig. 2.

Increasing the coupling further ($\mathcal{G}\sqrt{\langle n\rangle_0} > \pi$), we reach a regime of multistability (III). In this regime, the system can occupy either the original squeezed state, restricted by the first zero crossing of $\sin[\mathcal{G}(a^\dagger + a)]$, or a new squeezed state associated with the second or subsequent zeros in the sine function. Which of these states are occupied depends on which matrix elements are small, resulting in "hot spots" where the system (as a function of $\mathcal{G}$) suddenly jumps from one squeezed state to another, as can be seen in the bright regions of Fig. 2. Near the crossover between these states, the system displays bistability (and at higher $\mathcal{G}$ multistability) where the oscillator is in a statistical mixture of two squeezed states with distinct photon number distributions (the green curve in the inset of Fig. 2).

Measurement. A great advantage of the circuit-QED realization of a micromaser is that it is possible to make a time-resolved measurement of the microwave radiation
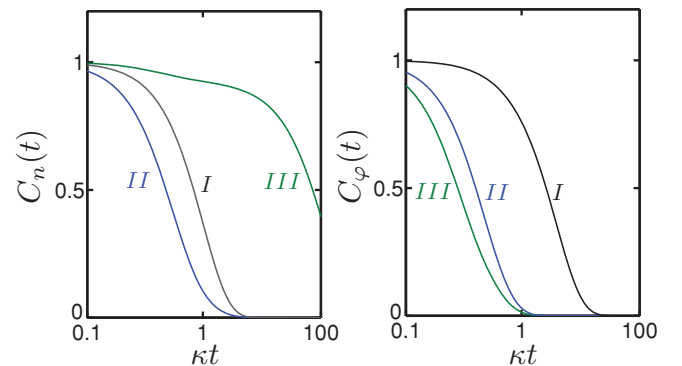
FIG. 3. (Color online) The amplitude C_n and the phase correlation function C_φ as a function of time, calculated from a numerical solution of the time evolution of the master equation (7). The different lines correspond to the different operating regimes shown in Fig. 2: black line I for $\mathcal{G} = 0.37$, blue line II for $\mathcal{G} = 0.93$, and green line III for $\mathcal{G} = 0.968$. We used the parameters $\kappa/\gamma = 0.027$ and $\mathcal{G}E_{JR}/\gamma = 6.7$.

emitted from the LC oscillator. Measuring the phase and the amplitude fluctuations makes it possible to distinguish among the different states of radiation in the cavity. Amplitude fluctuations are described by the amplitude correlation function,

$$C_n(t) = \frac{\langle a^\dagger(t)a(t)a^\dagger(0)a(0)\rangle - \langle a^\dagger a\rangle^2}{\langle (a^\dagger a)^2\rangle - \langle a^\dagger a\rangle^2} , \quad (10)$$

while phase fluctuations are given by the phase correlation function $C_\varphi(t) = \langle a^\dagger(t)a(0)\rangle/\langle a^\dagger a\rangle$. Both correlators have been normalized such that $C_i(0) = 1$ and they approach zero for long times, $C_i(t \to \infty) \to 0$. With this normalization, each correlator is fully characterized by a single decay rate, $C_i(t) \propto e^{-\kappa_i t}$. In Fig. 3 we show the amplitude and the phase correlation function for the LC oscillator in the various operating regimes. To calculate the phase correlator we solve Eq. (7) with the initial condition $\rho_\varphi(0) = a^\dagger \rho_{\rm st}$, where $\rho_{\rm st}$ is the stationary solution to Eq. (7). Similarly we find the amplitude correlator.

The two operating regimes II and III can be clearly distinguished in the amplitude correlation function. For a squeezed distribution (II), the amplitude is very similar at all times and therefore the amplitude decays very fast to its long-time limit. In contrast to this for a multistable distribution the field is fluctuating between two favored photon number states that are only connected by a small matrix element. Therefore it takes a long time until the amplitude correlator decays to its stationary value. The decay rates of the amplitude correlation function are therefore ordered such that $\kappa_n^{III} < \kappa_n^I < \kappa_n^{II}$. The decay rate of the coherent state lies between the two other decay rates as it is given approximately by the oscillator decay rate $\kappa_n^I \approx \kappa$. The coherent state can be distinguished through its very small phase correlation decay rate $\kappa_\varphi \propto 1/\langle n\rangle$.

Conclusion. We have presented a circuit design for creating nontrivial microwave photon distributions using a SSET strongly coupled to a strip-line or LC resonator. Using a combination of Cooper-pair tunneling and coupling to voltage fluctuation noise, a lasing cycle can be established. As this can be achieved while operating at a charge degeneracy point, the system is also better protected against low-frequency charge noise.

Realizing the strongly nonlinear coupling regime requires an oscillator with a large ratio of charging energy to inductive energy, $\mathcal{G} = (2\epsilon_C/E_L)^{1/4}$. Such an oscillator has been demonstrated in Ref. 20. A superconducting quantum interference device array was used as an effective resonator, which has the additional advantage of allowing for a tunable $\mathcal{G}$, such that all regimes discussed in this paper can be accessed in a single experiment. Another possible realization is to use a tunable right-hand (or left-hand) Josephson junction. This would allow one to change the photon number of the linear limit $\langle n\rangle_0$. An increase of the photon number would allow the measurement of all three regimes as well.

[1] A. Wallraff, D. I. Schuster, A. Blais, L. Frunzio, R.-S. Huang, J. Majer, S. Kumar, S. M. Girvin, and R. J. Schoelkopf, Nature (London) **431**, 162 (2004).

[2] T. Niemczyk *et al.*, Nature Phys. **6**, 772 (2010).

[3] J. Hauss, A. Fedorov, C. Hutter, A. Shnirman, and G. Schön, Phys. Rev. Lett. **100**, 037003 (2008).

[4] M. Grajcar, S. H. W. van der Ploeg, A. Izmalkov, E. Il'ichev, H.-G. Meyer, A. Fedorov, A. Shnirman, and G. Schön, Nature Phys. **4**, 612 (2008).

[5] D. A. Rodrigues, J. Imbers, and A. D. Armour, Phys. Rev. Lett. **98**, 067204 (2007).

[6] S. André, P.-Q. Jin, V. Brosco, J. H. Cole, A. Romito, A. Shnirman, and G. Schön, Phys. Rev. A **82**, 053802 (2010).

[7] D. Astafiev, K. Inomata, A. O. Niskanen, T. Yamamoto, Yu. A. Pashkin, Y. Nakamura, and J. S. Tsai, Nature (London) **449**, 588 (2007).

[8] M. Hofheinz *et al.*, Nature (London) **459**, 546 (2009).

[9] K. Moon and S. M. Girvin, Phys. Rev. Lett. **95**, 140504 (2005).

[10] M. Marthaler, G. Schön, and A. Shnirman, Phys. Rev. Lett. **101**, 147001 (2008).

[11] P. Filipowicz, J. Javanainen, and P. Meystre, Phys. Rev. A **34**, 3077 (1986).

[12] W. E. Lamb, W. P. Schleich, M. O. Scully, and C. H. Townes, Rev. Mod. Phys. **71**, S263 (1999).

[13] H. Walther, B. T. H. Varcoe, B.-G. Englert, and T. Beckert, Rep. Prog. Phys. **69**, 1325 (2006).

[14] O. Benson, G. Raithel, and H. Walther, Phys. Rev. Lett. **72**, 3506 (1994).

[15] M. Weidinger, B. T. H. Varcoe, R. Heerlein, and H. Walther, Phys. Rev. Lett. **82**, 3795 (1999).

[16] A. Maassen van den Brink, G. Schön, and L. J. Geerligs, Phys. Rev. Lett. **67**, 3030 (1991).

[17] J. Leppakangas and E. Thuneberg, Phys. Rev. B **78**, 144518 (2008).

[18] Y. Makhlin, G. Schön, and A. Shnirman, Rev. Mod. Phys. **73**, 357 (2001).

[19] M. O. Scully and M. S. Zubairy, *Quantum Optics* (Cambridge University Press, Cambridge, 1997).

[20] M. A. Castellanos-Beltran and K. W. Lehnert, Appl. Phys. Lett. **91**, 083509 (2007).